Evidence of spin scattering and collection of hot electrons at different conduction minima in Si

Parui, S.; Rana, K. G.; Banerjee, T.

Published in:
Applied Physics Letters

DOI:
10.1063/1.4819488

Evidence of spin scattering and collection of hot electrons at different conduction minima in Si

S. Parui, K. G. Rana, and T. Banerjee
Physics of Nanodevices, Zernike Institute for Advanced Materials, University of Groningen, Nijenborgh 4, 9747 AG Groningen, The Netherlands

(Received 25 July 2013; accepted 13 August 2013; published online 23 August 2013)

We observe unusual features in the bias dependence of spin transport in a Co/Au/NiFe spin valve fabricated on a highly textured Cu(100)/Si(100) Schottky interface, exploiting the local probing capabilities of a Ballistic electron magnetic microscope. This is ascribed to local differences in strain and the presence of misfit dislocations at the Schottky interface that enhances spin flip scattering and broaden the energy and angular distribution of the transmitted electrons. Cumulatively, these enable the transmitted hot electrons to probe the different conduction band minima in Si, giving rise to such bias dependent features in the magnetocurrent. [http://dx.doi.org/10.1063/1.4819488]

Metallic spin valves on Schottky interfaces are ideal for investigating spin transport in ferromagnetic (FM) layers, studying spin asymmetry of relaxation times for electrons and holes in FMs, probing spin-sensitivity of transmission at the electronically dissimilar FM-Semiconductor (SC) hetero-interface, etc. This is exemplified by numerous studies involving hot electron transport in metallic spin valves on different conventional semiconductors as Si,[1–9] GaAs,[10,11] GaP,[12] GaAsP,[13] etc. Probing a different regime of the electronic band structure, such studies involving hot electrons and holes have yielded quantitative estimates of different transport parameters as the scattering time and attenuation length at energies a few eV above and below E_F,[14] and have been utilized for designing new schemes and devices in spintronics. Studies on spin transport reported so far have been performed using spin valves with different FMs as NiFe, Co, Fe, etc., on polycrystalline Schottky interfaces with Si. In GaAs, a *direct* band gap semiconductor, epitaxial Schottky interfaces are formed with Fe or its alloys and spin dependent transmission has revealed nonmonotonic bias dependence of the magnetocurrent (MC) arising from the different conduction band structures in GaAs.[10,11]

Although hot electrons have been widely used to study spin dependent transport in ferromagnets,[5–9] spin filtering of hot electrons in a spin valve has not been utilized earlier for probing the local band structure of an *indirect* band gap semiconductor in a spintronic device. Here, we demonstrate a unique approach of exploiting hot electron spin transport in a Co/Au/NiFe spin valve grown on a highly textured Schottky interface of Cu(100)/Si(100) that reveals signatures of the electronic structure of an indirect band gap semiconductor of Si(100). This is demonstrated by analyzing the collected current, on the nanoscale, at different regions of the textured Schottky interface using the local probing capabilities of the Ballistic electron magnetic microscope (BEMM).[5,6,15,16] Although it is known that ultrathin Cu grows epitaxially on Si(100),[18–20] such interfaces have not been exploited earlier to study spin dependence of transmission in metallic spin valves at the nanoscale. Interestingly, for different locations in the same spin valve device on Si(100) (denoted as regions 1 and 2), we find that the collected current for both parallel (I_P) and antiparallel (I_{AP}) alignments of the magnetic layers exhibit significant differences in their bias dependence. The overall transmission for I_P, in region 2 (R2) is generally found to be lower than in region 1 (R1) up to a bias of ~ -1.4 V and thereafter increases gradually. For the antiparallel case, the increase is more abrupt at a similar bias. Further, the collected current in R2 exhibits unusual features in its bias dependence beyond ~ -1.4 V. A large MC of ~500% (at -0.9 V) [MC $= (I^P - I^{AP})/I^{AP}$] is predominantly observed (in R1), which decreases to ~170% (at -2 V) with a monotonic bias dependence. The extracted magnetocurrent in R2 also decreases and reaches ~100% at -2 V.

To study the bias dependence of spin transport, we have used BEMM. BEMM is a three electrode extension (Fig. 1)

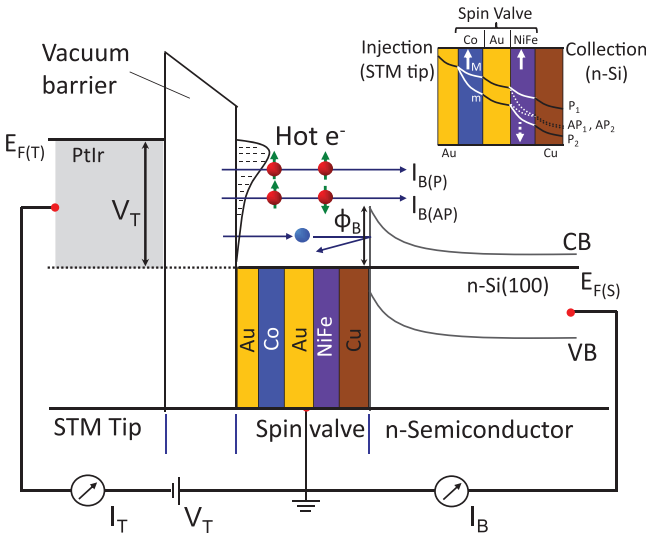

FIG. 1. Schematic energy diagram of the BEMM experiment. The sample consists of a n-Si(100) substrate coated with Cu(10)/NiFe(4)/Au(10)/Co(4)/Au(5) (nm). The STM tip is used to locally inject hot electrons into the multilayer base by tunneling at a bias voltage V_T between tip and Au surface. The current I_B flows perpendicular through the stack and is collected at the conduction band of the Si substrate. Top right shows spin-dependent transmission of the majority and minority electrons at the normal metal/ferromagnetic metal interface and their exponential decay in the bulk of the metal films. The P and AP transmissions are described in Eqs. (1) and (2).

of the Scanning tunneling microscopy (STM) that is used to investigate perpendicular spin transport through buried layers and interfaces in a spin valve grown on a semiconducting substrate.[5–7] A PtIr STM tip is used to locally inject electrons onto the top Au layer and an additional contact at the semiconductor rear serves as the collector.[15,16] In BEMM, the energy of the injected electrons can be varied by changing the applied bias V_T for a fixed tunnel current I_T. The spin dependence of the collected current, I_B, is obtained by applying a magnetic field that changes the relative magnetization alignment of the FM layers in the spin valve. After transmission through the spin valve, the electrons are collected in the conduction band of the Si semiconductor, provided they satisfy the necessary energy and momentum criteria at the M/S Schottky interface. The spin dependent collector current, I_B, for the parallel and antiparallel configuration, can be written as,

$$I_B^P \propto (T_{FM1}^M T_S T_{FM2}^M + T_{FM1}^m T_S T_{FM2}^m)\Upsilon_{Cu/Si}^P, \quad (1)$$

$$I_B^{AP} \propto (T_{FM1}^M T_S T_{FM2}^m + T_{FM1}^m T_S T_{FM2}^M)\Upsilon_{Cu/Si}^{AP}, \quad (2)$$

where T^M and T^m refer to the transmission of the majority (M) and minority (m) hot electrons in the ferromagnetic layers, and T_S is the transmission in the spacer (non-magnetic, NM) layer. The bulk transmission depends exponentially on the NM and FM layer thickness as, $T \propto e^{-d/\lambda}$, where d is the thickness and λ is the hot electron attenuation length for the NM and FM layers [see inset of Fig. 1]. $\Upsilon_{Cu/Si}$ denotes the scattering sensitive transmission probability at the highly textured M/S interface.

For the BEMM experiments, we use n-type Si(100) substrate (the carrier concentration of n-Si is 10^{15} cm^{-3}) with a 300 nm thick SiO_2, which is removed by buffered hydrofluoric acid (HF). The pre-defined circular devices, 150 μm in diameter, are hydrogen terminated using 1% hydrofluoric acid, onto which metal layers were deposited by e-beam evaporation. First, a 10 nm Cu layer was evaporated to form a highly textured Cu/Si Schottky barrier,[18,19] followed by the deposition of 4 nm of NiFe, 10 nm of Au, and 4 nm of Co films. A final 5 nm of Au film serves as a capping layer, for *ex situ* sample transfer to the BEMM set up. We have used x-ray diffraction (XRD) to study the growth of Cu film evaporated on hydrogen terminated n-Si(100). From the diffraction peaks, the in-plane lattice constants are extracted to be 0.3615 nm for Cu and 0.5431 nm for Si. This yields a lattice mismatch of 33% along (100), but decreases to 6% if the Cu(100) rotates 45° with respect to Si(100) plane as discussed in Refs. 18 and 19 (further details in the supplementary information[21]).

For an unambiguous demonstration of spin transport in such spin valves, nanoscale magnetic hysteresis loops were recorded using BEMM as shown in Fig. 2(a). The magnetic field dependence of the transmission measured at −2 V and 4 nA tunnel injection shows clear switching, characteristic of the relative parallel and antiparallel alignment of the NiFe and Co layers. A typical measurement starts by fully saturating and aligning the magnetization of both the FMs by ramping the magnetic field to a maximum. When the magnetic field is swept through zero and changes sign, the softer FM viz. NiFe switches, leading to an anti-parallel (AP) alignment and reduction in BEMM current. A further increase in the magnetic field switches the Co layer along the magnetization direction of the NiFe layer, defining a parallel (P) alignment and resulting in a higher BEMM current. The inset confirms independent switchings of the NiFe and Co layers in the spin

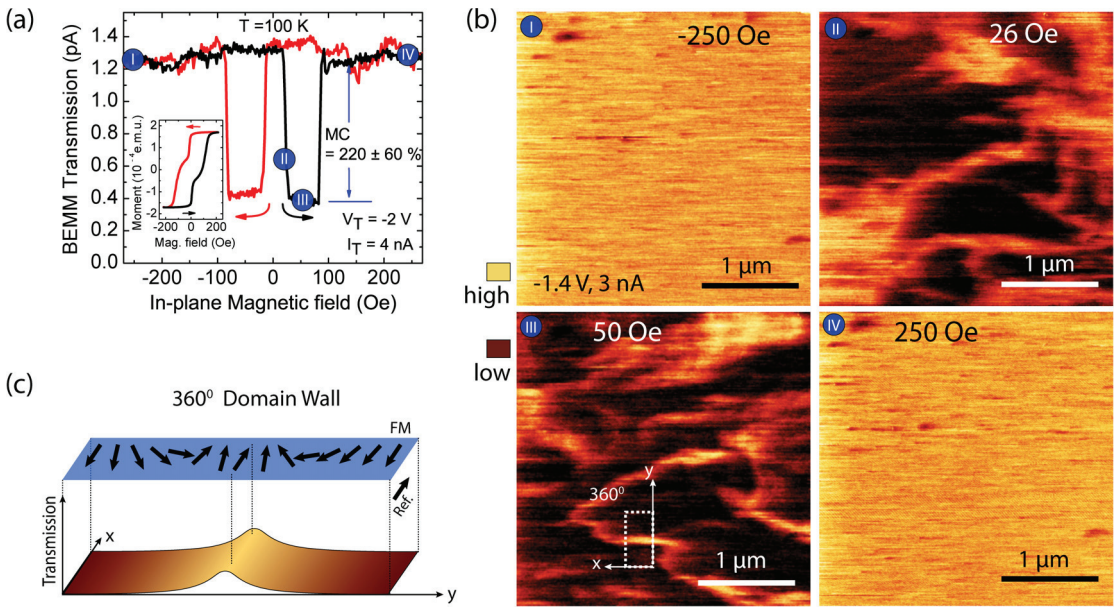

FIG. 2. (a) Local hysteresis loop obtained by BEMM at V_T of −2 V and at I_T of 4 nA, showing clear P and AP transmissions. NiFe switches at ∼16 Oe and the switching field of Co on Au is at ∼86 Oe. These values are consistent with that obtained from SQUID measurement. (Inset) SQUID magnetometer measurement exhibits hysteresis loops with well-defined plateaus representing anti-parallel configuration of Co and NiFe magnetic moments. (b) Series of magnetic images are recorded as the BEMM transmission by scanning the tip over a fixed 3×3 μm^2 area at V_T of −1.4 V and at I_T of 3 nA. Obtained BEMM images are shown in (I), (II), (III), and (IV) for the in-plane magnetic field values of −250, 26, 50, and 250 Oe, respectively. BEMM current ranges from 0.56 pA (light) to 0.12 pA (dark) as standard P and AP states. (c) 360° domain wall is represented schematically as is observed in the AP state mixed with local P state indicated in the white box in Fig. 2(b) (III). A full 360° rotation of the magnetization gives rise to such domain walls in one of the ferromagnet relative to the other.

valve, using Superconducting Quantum Interference Device (SQUID) and characterized by a stepped hysteresis loop with two distinct coercive fields,[22] matching well with that of the magnetic hysteresis loop obtained using BEMM.

Figure 2(b) shows a series of collected electron current images obtained by scanning the tip across a $3 \times 3\,\mu m^2$ area on the n-Si/Cu(10)/NiFe(4)/Au(10)/Co(4)/Au(5) (all thickness in nm) structure at different applied magnetic fields. Magnetic images are recorded at V_T of -1.4 V, I_T of 3 nA and the obtained images are shown in (I), (II), (III), and (IV) for the in-plane magnetic field values of -250, 26, 50, and 250 Oe, respectively. The color contrast in the images are such that the bright part represents BEMM current in the P state, while the dark part represents BEMM transmission in the AP configuration. The magnetization of both the FMs is saturated at a field of -250 Oe and (I) corresponds to a large hot electron transmission corresponding to the P state. The magnetic field is then decreased to zero and reversed to a small positive value. At a field of 26 Oe, magnetic contrast appears defining a local AP magnetic state that coexists with regions of large electron current. Increasing the magnetic field results in the evolution of the AP state with a reduction in the BEMM current. However, in (III) we observe an inhomogeneous BEMM transmission due to the presence of magnetic domains. We observe 360° domain walls[9,17] that act as a nucleation centre for magnetization reversal. At higher magnetic fields of 250 Oe, as shown in (IV), the domain walls annihilate and the entire region exhibits a large BEMM transmission corresponding to the parallel state. Fig. 2(c) illustrates the formation of 360° domain walls where the magnetization in one ferromagnet rotates 360° in-plane, relative to the other ferromagnet. Magnetic resolution using one such 360° domain wall was reported to be 16 nm,[23] in a recent work. For the BEMM transmission studies, the STM tip was placed at several locations in the device (chosen at random) and the transmission for both P and AP states was recorded for each particular tip position.

Spin-dependent transmission as measured in BEMM for both parallel and anti-parallel magnetization orientations of the NiFe(4)/Au(10)/Co(4) spin valve is shown in Figs. 3(a) and 3(b). Figure 3(a) represents the transmission as obtained in approximately 90% of the device area in n-Si/Cu(10)/NiFe(4)/Au(10)/Co(4)/Au(5) and designated as R1. However, by moving the STM tip across the device, the BEMM transmission as well as the spectral shape is found to differ (as shown in Fig. 3(b)), at few other locations (approximately 10% of the device area), from that in R1, and denoted here as R2. At such locations, we also observe unusual features in the bias dependence for both the I_P and I_{AP} transmissions. The overall transmission for I_P is lower than that in R1 up to a bias of ~ -1.4 V and thereafter increases gradually. For the antiparallel case, the increase is more abrupt at a similar bias. The spectral shape of the collected current for the parallel and antiparallel transmission reflects the narrow energy distribution of the transmitted majority electrons and a relatively broad one for the minority electrons. The extracted magnetocurrent for the two regions is shown in Fig. 3(c). The MC decreases with bias for both the regions but is more abrupt for R2 and reaches $\sim$100% at -2 V. To rule out possible artifacts in the BEMM transmission related

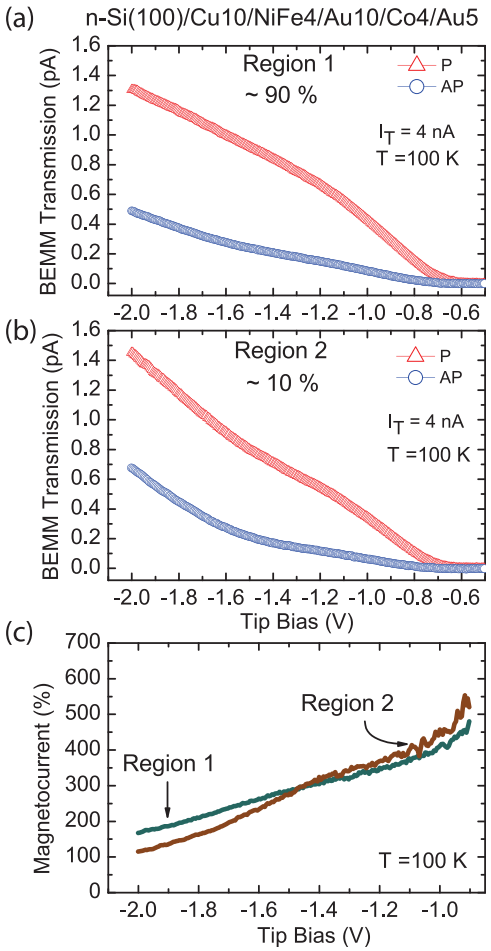

FIG. 3. (a) and (b)The variation of the BEMM transmissions for parallel (P) and anti-parallel (AP) magnetization configuration of the Si/Cu(10)/NiFe(4)/Au(10)/Co(4)/Au(5) device corresponding to two different regions in the same device. For both regions, the transmission is larger for P than of AP state. In region 2, a second onset is found at above ~ -1.4 V for both P and AP transmissions unlike that in region 1. (c) From the parallel and antiparallel BEMM transmission, magnetocurrent is extracted for both regions 1 and 2 and plotted with respect to the bias.

to the growth, we have also fabricated and measured spin dependent transport in a n-Si/Cu(10)/Co(4)/Au(10)/NiFe(4)/Au(5) device (i.e., the bottom FM is now Co). Here too (supplementary Figure S1, Ref. 21), we find the occurrence of two regions with a similar transmission characteristics and bias dependence of MC (Fig. S1). Direct visualization of such features as observed in I_P and I_{AP} is difficult to obtain from the BEMM images, due to challenges involved in the clear isolation of the possible origin of local magnetic contrast in these images (as local differences in the thickness of the buried thin films in the spin valve, etc.).

The non trivial bias dependence of the BEMM transmission is further analyzed in Fig. 4. It shows the data of the BEMM transmission for P and AP configurations, in regions 1 and 2, normalized to its value at -2 V (left) and -1.2 V (right). We find that the spectral shape and the energy dependence of the BEMM transmission in R2 are different than in R1, for both the P and AP alignments, when normalized at -2 V. Normalizing the transmissions at a lower energy allows us to identify the onset in the bias beyond which features in the P and AP spectra set in. This has been done at several lower biases and is shown for a bias of

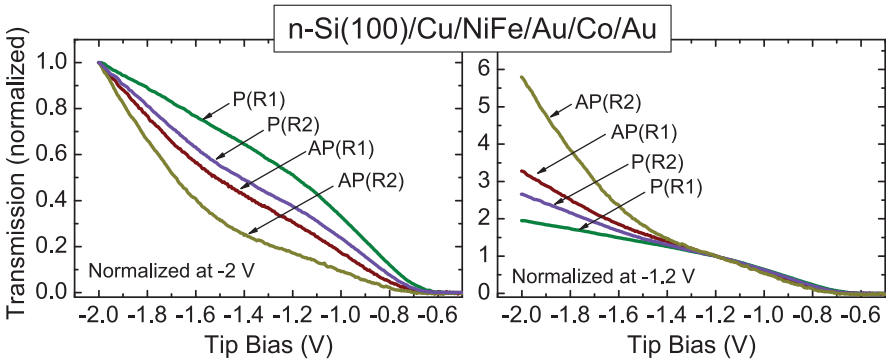

FIG. 4. Normalized transmissions for the Si/Cu(10)/NiFe(4)/Au(10)/Co(4)/Au(5) device from Fig. 3. Both the P and AP transmissions are normalized at tip biases of −2 V (left) and −1.2 V (right), respectively. Normalized plots at −2 V show a distinct change in the direction of curvatures indicating different energy dependence for region 2. When the BEMM transmissions are normalized at −1.2 V, the onset of the energy dependence of the transmissions becomes more pronounced, as shown around −1.4 V.

−1.2 V (Fig. 4 right). We see that beyond ∼ −1.4 V, the energy dependence of both the P and AP transmissions becomes more pronounced and correspond to the energy beyond which the unusual features in the BEMM transmission set in.

The spin dependence of transmission of the injected electrons propagating through the spin valve stack ($T^{M,m}_{FM1,2}$) and their interfaces are expected to be similar in both regions 1 and 2 of the device. However, inhomogeneity at the M/S interface in the device, due to local differences in the strained epitaxial lattice and/or the presence of misfit dislocations acts as effective elastic scattering centers, as in R2, and increases the transmission probability ($\Upsilon_{Cu/Si}$) of the transmitted electrons, above ∼ −1.4 V, at such M/S interfaces. These scattering events also broaden the energy and angular dependence of the transmitted electrons and increase the relative fraction of minority electrons by spin flip processes at the interface (increase in I_{AP}). This is accompanied by a concomitant reduction in the spin asymmetry (I_P/I_{AP}) at higher energies (above ∼ −1.4 V) and is manifested as an abrupt decrease in the MC with bias in R2. Such features are thus observed only with a spin valve layer stack and not for single ferromagnetic layers. Subsequently, this energy and momentum broadening of the transmitted electrons enables the electrons with larger parallel wave vectors to access the almost degenerate minima of the second conduction band in addition to the first conduction band at the X point (85% from the Γ point) in Si, besides probing the second minima in the first conduction band at the L point as shown in Fig. 5. The unusual features observed in the bias dependence of spin transport in R2 correspond well to these additional thresholds in the conduction band minima in Si at both the X (corresponds to collection from and above the Schottky barrier height of 0.62 eV at the Cu/n-Si(100) interface[20]) and L point (corresponds to ∼0.8 V above the Schottky barrier height).[24,25] Thus, the observed effect at ∼ −1.4 V is 0.8 V above the Schottky barrier height at the M/S interface and matches with the energy separation between the first conduction band minima at X and the second conduction band minima at L in Si.

This possibility to probe additional conduction band minima in an indirect band gap semiconductor as Si was not demonstrated in earlier studies involving polycrystalline M/S interfaces. It is enabled by the unique choice of an epitaxial M/S interface and the capabilities of the BEMM in resolving spatial differences in spin transport, in the same device, that arises due to differences in the local strain at the underlying epitaxial oriented Cu/Si interface. The local differences in the epitaxial oriented Cu/Si interface due to misfit dislocations in R2 enhance momentum scattering and broaden the energy and angular distribution of the transmitted electrons. This, in turn, increases the minority electrons due to spin flip processes, decreases the transmission asymmetry at higher energies, and reduces the MC. All these cumulatively enables the hot electrons with larger parallel wave vectors to access the X and L bands in an indirect band gap material as Si giving rise to such features in their spin transport, hitherto not reported, and is an interesting approach to probe the electronic band structure in semiconductors.

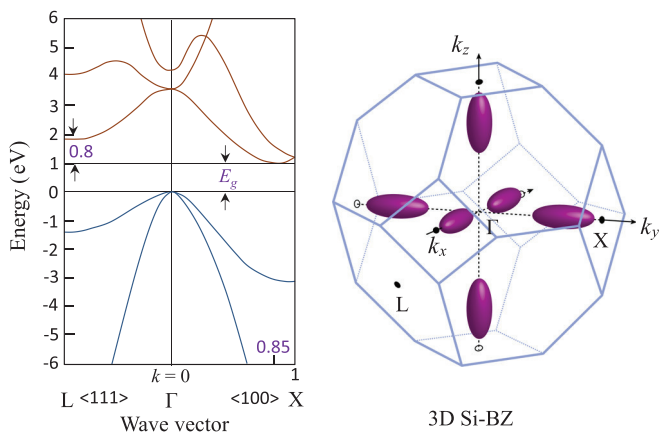

FIG. 5. There are six equivalent ellipsoidal first conduction band minima at X, which is at a distance about 85% from the Γ point. The second conduction band minima are only 0.1 eV above the minima of the first conduction band at the X-points. The second minima of the first conduction band are at the L points, which are about 0.8 eV above the first minima. There are eight such L minima (not shown in 3D Si-BZ), which contribute to the extra collection of scattered hot electrons above the second onset (SBH + 0.8 ≈ 1.4 eV).

We thank A. M. Kamerbeek for useful discussions, T. T. M. Palstra and B. Noheda for use of the XRD and SQUID. Technical support from J. Holstein, J. Baas, B. Wolfs, and M. de Roosz is thankfully acknowledged. This work was financially supported by the NWO-VIDI program, the Zernike Institute for Advanced Materials and NanoNed program coordinated by the Dutch Ministry of Economic Affairs.

[1]D. J. Monsma, R. Vlutters, and J. C. Lodder, Science **281**, 407 (1998).
[2]D. J. Monsma, J. C. Lodder, Th. J. A. Popma, and B. Dieny, Phys. Rev. Lett. **74**, 5260 (1995).
[3]I. Appelbaum, B. Huang, and D. J. Monsma, Nature (London) **447**, 295 (2007).

[4]B. Huang, D. J. Monsma, and I. Appelbaum, Phys. Rev. Lett. **99**, 177209 (2007).
[5]W. H. Rippard and R. A. Buhrman, Appl. Phys. Lett. **75**, 1001 (1999).
[6]W. H. Rippard and R. A. Buhrman, Phys. Rev. Lett. **84**, 971 (2000).
[7]T. Banerjee, J. C. Lodder, and R. Jansen, Phys. Rev. B **76**, 140407(R) (2007).
[8]T. Banerjee, W. G. van der Wiel, and R. Jansen, Phys. Rev. B **81**, 214409 (2010).
[9]A. Kaidatzis, S. Rohart, A. Thiaville, and J. Miltat, Phys. Rev. B **78**, 174426 (2008).
[10]S. van Dijken, X. Jiang, and S. S. P. Parkin, Phys. Rev. Lett. **90**, 197203 (2003).
[11]X. Jiang, S. van Dijken, R. Wang, and S. S. P. Parkin, Phys. Rev. B **69**, 014413 (2004).
[12]C. V. Reddy, R. E. Martinez II, V. Narayanamurti, H. P. Xin, and C. W. Tu, Phys. Rev. B **66**, 235313 (2002).
[13]E. Heindel, J. Vancea, and C. H. Back, Phys. Rev. B **75**, 073307 (2007).
[14]T. Banerjee, E. Haq, M. H. Siekman, J. C. Lodder, and R. Jansen, Phys. Rev. Lett. **94**, 027204 (2005).
[15]W. J. Kaiser and L. D. Bell, Phys. Rev. Lett. **60**, 1406 (1988).
[16]L. D. Bell and W. J. Kaiser, Phys. Rev. Lett. **61**, 2368 (1988).
[17]E. Haq, T. Banerjee, M. H. Siekman, J. C. Lodder, and R. Jansen, Appl. Phys. Lett. **86**, 082502 (2005).
[18]H. Jiang, T. J. Klemmer, J. A. Barnard, and E. A. Payzant, J. Vac. Sci. Technol. A **16**, 3376 (1998).
[19]B. G. Demczyk, R. Naik, G. Auner, C. Kota, and U. Rao, J. Appl. Phys. **75**, 1956 (1994).
[20]S. Parui, J. R. R. van der Ploeg, K. G. Rana, and T. Banerjee, Phys. Status Solidi (RRL) **5**, 388 (2011).
[21]See supplementary material at http://dx.doi.org/10.1063/1.4819488 for fabrication and spin transport studies on a different spin-valve and its non-trivial bias dependence.
[22]T. Luciński, S. Czerkas, H. Brückl, and G. Reiss, J. Magn. Magn. Mater. **222**, 327 (2000).
[23]S. Parui, K. G. Rana, and T. Banerjee, in 2012 IEEE International Electron Devices Meeting (IEDM) (2012), pp. 11.4.1–11.4.4.
[24]M. L. Cohen and T. K. Bergstresser, Phys. Rev. **141**, 789 (1966).
[25]C. S. Wang and B. M. Klein, Phys. Rev. B **24**, 3393 (1981).